ORIGINAL PAPER

Eur. J. Histochem.
44: 419-432, 2000

Wavelength dependence of the time course of fluorescence enhancement and photobleaching during irradiation of ethidium bromide-stained nuclei

L. Galassi

University of Naples, Department of Zoology, Via Mezzocannone 8, I-80134 Napoli, Italy

Accepted: 11/07/00

Key words: fluorescence enhancement, microspectrofluorimetry, photobleaching

SUMMARY

The variation of fluorescence during irradiation of ethidium bromide-stained nuclei with the 458 nm argon laser line was measured at different wavelengths throughout the emission spectrum. When glycerol was used as a mountant, photoenhancement of fluorescence was observed at all wavelengths, but was greater at the shorter wavelengths. Fluorescence increased by almost one order of magnitude at 500 nm after 40 s of irradiation, compared with only about 10% at wavelengths longer than 600 nm after 2-3 s. In nuclei mounted in phosphate buffer, an initial photoenhancement of fluorescence was detected only at the shorter wavelengths, while continuous photobleaching was observed in the rest of the emission spectrum. When the spectra are normalized to maximum, so as to eliminate the effect of the concurrent photobleaching, it appears that the difference between the time course of fluorescence variation in buffer and glycerol depends largely on the lower photobleaching rate in glycerol. The photoenhancement of fluorescence at shorter wavelengths was found to consist of a band peaking at 485-491 nm in glycerol and at 495-496 nm in buffer. Attenuation of the inner-filter effect contributes minimally to the enhancement of fluorescence at shorter wavelengths. Since the dimer is known to be non fluorescent, the light-induced disaggregation of dimers to monomers cannot be an explanation for the large increase of fluorescence at the shorter wavelengths. The same laser beam that was used to excite the fluorescence of stained nuclei was also used for monitoring the concomitant variation of transmitted light, from which the variation of absorptance during irradiation was computed. While the expected decrease of absorptance was observed in glycerol, reflecting the photodestruction of the fluorophore, in buffer solution an unexpected initial increase was found, which may reflect the accumulation of an absorbing photoproduct.

INTRODUCTION

Although the time course of fluorescence photobleaching can generally be ascribed to mono-exponential photo-destruction of fluorophores, in microfluorimetry discrepancies from simple mono-exponential kinetics have been reported in the past by several authors (Benson *et al.*, 1985; Bjarneson and Petersen, 1991; Szabò, 1992; Brakenhoff *et al.*, 1994; Song *et al.*, 1995, 1996, 1997; Van Oostveldt

Correspondence to: L. Galassi
E-mail: galassi@unina.it

et al., 1998). The most extreme deviation from the expected kinetics is represented by the photo-enhancement of fluorescence observed immediately after the onset of illumination (West and Lorinez, 1973; Enerback, 1974; Severin and Ohnemus, 1982; Ruck *et al.*, 1990; Peng *et al.*, 1991; Ambroz *et al.*, 1994; Galassi, 1996). Discrepancies between variation of fluorescence and photo-destruction have recently been reported in macro-fluorimetric studies as well. When the quantum yield of the photo-bleaching rate of porphyrins was compared with the variation in absorbance (Bezdetnaya *et al.*, 1996), it was found to be an order of magnitude higher. Also, the rate of mTHPC photo-degradation, monitored by decay in absorbance, was found to be fifteen-fold lower than the rate of loss of fluorescence (Bilitchenko *et al.* 1998). The correlation of fluorescence fading with decrease of absorbance thus appears not to be straightforward, because of possible variations of the fluorescence quantum efficiency during irradiation, due to light-induced modification of the fluorophore–fluorophore interactions (photo-dimerisation or disegregation), fluorophore–substrate interactions, or fluorophore–solvent interactions. Photo-products may also be formed which absorb at the wavelength of the excitation light.

It was, therefore, of interest to compare the variation of fluorescence at different emission wavelengths vs. absorption during laser irradiation of ethidium-stained nuclei, which show an initial photo-enhancement of fluorescence (Galassi,1996). Continuous measurement of fluorescence and transmitted light during irradiation was chosen in preference to end-point measurements, since the latter method cannot account for possible reversal events taking place between completion of irradiation and making the final measurement. (Rundquist and Enerback, 1976; Scalatter *et al.*, 1990, Stout and Axelrod 1994, 1995, Periasamy *et al.*, 1996; Swaminathan *et al.*, 1996, 1997, Azizi and Wahl, 1997).

Contrary to the common assumption that bleaching affects all wavelengths of the emission spectrum equally, West and Lorinez (1974) first observed marked differences in the variation of fluorescence intensity of acridine orange-stained leukocytes depending on the emission wavelength, with fluorescence photo-enhancement occurring at 530 nm and photo-bleaching at 660 nm. Ethidium bromide-stained nuclei mounted in glycerol, but not when mounted in buffer, were reported to undergo photo-enhancement of fluorescence when fluorescence was measured over the entire emission spectrum (Galassi, 1996). When measurements are taken with no band filtering, variations taking place in the tails of the spectrum are overwhelmed by the high intensities of light around the peak wavelengths. The shortest wavelengths are especially affected, because of the S-shaped LP filter transmittance cut-off in this region. The data to be presented here show that fluorescence of ethidium, measured at the shortest wavelengths of the emission spectrum, displays a remarkable photo-enhancement in buffer solution as well as in glycerol, and the photo-enhancement in glycerol is much higher then when the whole emission spectrum is measured.

MATERIALS AND METHODS

Cells and staining

Blood smears of *Rana esculenta* L. were fixed in methanol and stained with ethidium bromide (Sigma, St.Louis, MO, USA) in 0.02 M phosphate buffer, pH 7.0, at a dye concentration of 3×10^{-4} M, for 1 h at 20°C. They were rinsed with phosphate buffer (three washes of 5 min each) and mounted either in the buffer solution or, after blotting, in glycerol (99.9% Aldrich, Steinheim, Germany). The staining baths were prepared from a stock solution of ethidium bromide in dimethyl sulphoxide (5 mg/ml, stored at 4°C in the dark). Concentration of the dye was determined spectrophotometrically from a dilute aqueous solution, using a molar extinction coefficient of 5850 M^{-1} cm^{-1} at 480 nm (Guenza and Cuniberti, 1988).

Instrumentation set-up

Figure 1 shows the instrumentation set-up. The microspectrofluorimeter was a Leitz MPV2 (Ernst Leitz, Wetzlar, Germany) equipped with an EMI 9558A photomultiplier tube (Channel 1). The light source was a multiline 100 mW Argon laser (American Laser, Salt Lake City, Utah, USA). The light power at the exit pupil of the microscope objective was measured with a calibrated power meter (Newport, Irvine, California, USA), and expressed as mean intensity (i.e. power/μm^2) of the field diaphragm area (316 μm^2) at the focal plane.

Ahead of the dichroic beam-splitter a quartz light sampler split a small amount of light to an ampli-

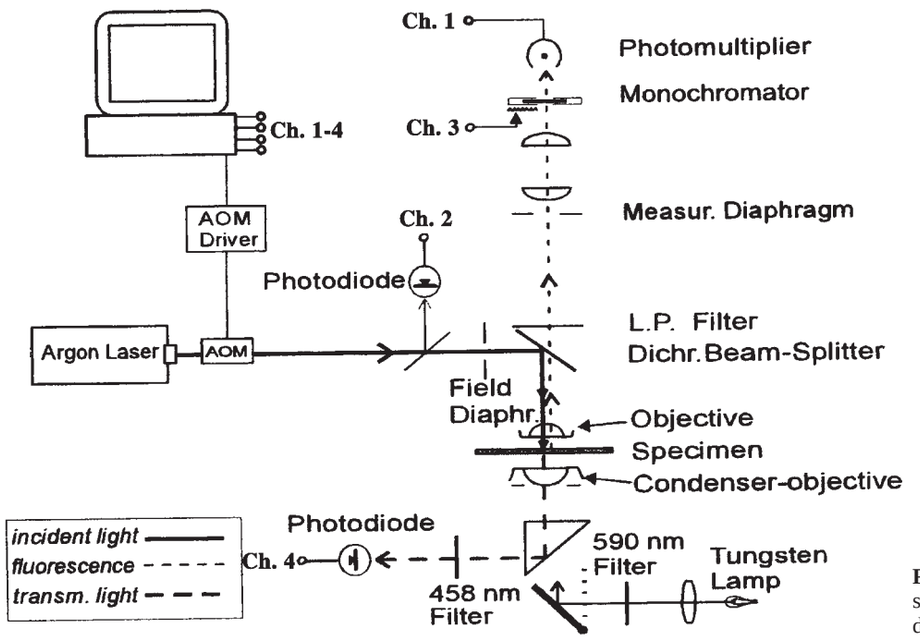

Fig. 1 - Instrumentation set-up. See text for a full description. Ch = channel.

fied photodiode (Thorlabs, Newton, N.J., USA), which was used to correct for light instabilities (Channel 2). The 457.9 nm laser line, selected with the built-in prism, was used for excitation. This short wavelength, within the excitation spectrum of ethidium, together with an RKP455 dichroic beam splitter and a 490 LP filter, allowed emission measurements down to 468 nm with virtually no reflected excitation light reaching the photomultiplier (Galassi, 1990). The excitation light was focused on to the sample, and the fluorescent light collected, with a x90/1.32 NA objective.

Spectra were obtained with a motorised (16.2 nm/s scan speed) Veril continuous interference monochromator (FWHM 24.8 nm at 458 and 25.1 nm at 632 nm). The argon laser lines and the 632.8 nm line of a HeNe laser (Spectra-Physics, Mountain View, California, USA) were used for calibrating the monochromator wavelength potentiometer output (Channel 3) and determining the monochromator slit bandwidth.

Simultaneous monitoring of fluorescence and transmittance variations

The excitation light partly absorbed by the sample was collected with a Leitz x60/ 0.65 NA condenser-objective (Ernst Leitz, Wetzlar, Germany) and projected on to the head of a photodiode (Newport, Irvine, California, USA) through a 456 nm interference filter (Omega Optical, Brattleboro, Vermont, USA), which passed only the laser excitation line and blocked the fluorescence light (transmitted light measurements: Channel 4).

When dealing with chromophores having an irregular distribution and relatively high local extinctions, as is the case for nuclear probes in microfluorimetry, the relationship between the variation of mean absorbance and the variation of fluorescence is a complex one, depending on the degree of heterogeneity of the local extinctions, and in the case of laser illumination, on the gaussian distribution of irradiation. *Absorptance* ($\beta = 1-T$), unlike *extinction* ($\log(1/T)$), is, in principle, linearly related to fluorescence up to relatively high local concentrations (at which self-absorption of fluorescence would become significant) and, most importantly in cytofluorimetry, the linearity holds regardless of the spatial distribution of the fluorophore or the heterogeneity of illumination of the microscope field. In fact, for a microscope field containing i areas, each with illumination intensity I_{oi} and transmitted light intensity I_i, the measured absorptance is

$$\beta = 1 - \frac{\sum_i \mathrm{I}_i}{\sum_i \mathrm{I}_{oi}} = 1 - \frac{\mathrm{I}}{\mathrm{I}_{oi}}$$

where I and I_o are the light intensities measured through an area containing a stained nucleus and an empty area respectively. The fluorescence intensity is

$$F = \sum_i F_i = \mathrm{A}\sum_i \left(\mathrm{I}_{oi}\left(1 - \frac{\mathrm{I}_i}{\mathrm{I}_{oi}}\right)\right) = \mathrm{A}\left(\sum_i \mathrm{I}_{oi} - \sum_i \mathrm{I}_i\right) =$$

$$= \mathrm{A}\left(\sum_i \mathrm{I}_{oi}\right)\left(1 - \frac{\sum_i \mathrm{I}_i}{\sum_i \mathrm{I}_{oi}}\right) = \mathrm{A}\mathrm{I}_o\beta$$

A being a factor related to the quantum efficiency of the fluorophore and the instrumental response, the latter being constant during all the measurements.

Nuclei were localised using a tungsten-halogen lamp as the light source. A low illumination level and an interference filter 591/14 (at which wavelength the absorption by ethidium is very low) ensured virtually negligible fading during the search and focusing period. The tungsten lamp was later turned off and the dark currents were fed through a 12 bit 30 kHz A/D converter to a PC. After 0.1 s of dark current storage, the driver of an AOM (Crystal Technology, Palo Alto, California, USA), activated by the computer program, diverted the first order (+1) diffracted beam into the aperture of the field diaphragm, and the signals from channels 1, 3 and 4 were read.

The digitised fluorescence and transmitted light values were corrected for dark current and light instabilities, and were normalised relative to the gains of the photomultiplier, photodiode, and A/D converter. For graphic display, the data were divided in 100 groups and the mean was calculated for each group. In order to resolve the early variations in fluorescence intensity, which are usually very rapid, the first single readings, after AOM opening, were set as the initial point of the curves, at zero time. Each fluorescence curve shown in this paper was the average, point by point, of three acquisitions. Each absorptance curve is the average of at least ten acquisitions.

Acquisition and correction of emission spectra

The procedure for obtaining difference spectra between time *t* and time 0 was the following. Fifty duplicate recordings of fluorescence, lasting 40 s after the onset of illumination, were taken at fixed wavelengths, equally spaced from 468 to 760 nm. For each wavelength, the relative difference between the fluorescence intensity at time 0 (actually within 10^{-4} s from the onset of illumination, corresponding to the acquisition time of the A/D converter at a frequency of 10 kHz per channel) and at time *t* was determined. Smoothed difference spectra were constructed from these values by locally weighted polynomial fitting. The procedure for obtaining and correcting emission spectra was the

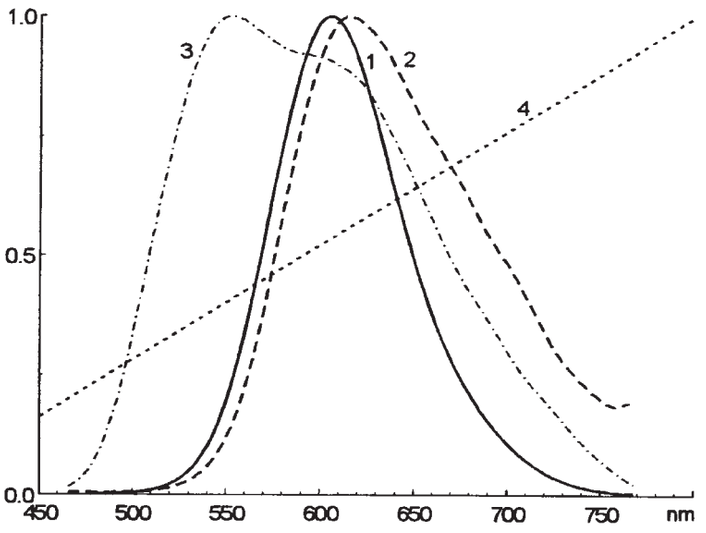

Fig. 2 - Curve 1: Measured emission spectrum of ethidium-stained nuclei mounted in glycerol, corrected only for fluorescence light-induced variations during monochromator scanning. Curve 2: Same spectrum corrected for instrumental response. Curve 3: Spectral response to a 3300°K colour temperature reference tungsten lamp of the instrument equipped with RKP455 dichroic beam splitter and LP490 filter. Curve 4: Relative spectral concentration of tungsten at 3300°K.

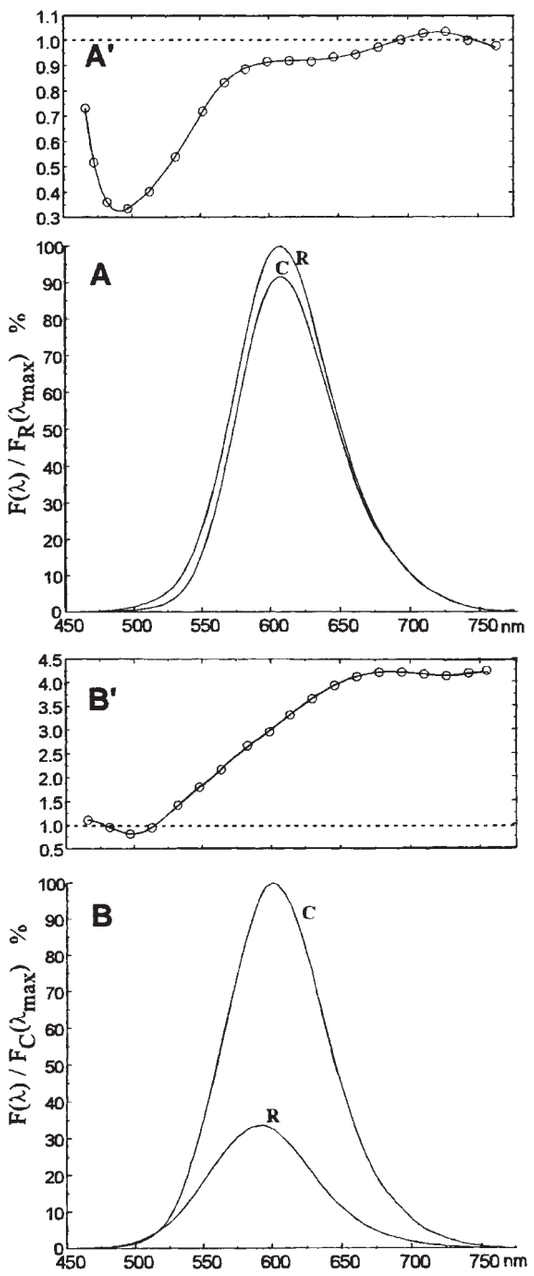

Fig. 3 - Emission spectrum of ethidium-stained nuclei mounted in glycerol (A) and phosphate buffer (B). R: Raw spectrum of ethidium bromide-stained nuclei. C: Same spectrum corrected for distortion caused by light-induced variation of fluorescence during monochromator scanning. A' and B' show the relative difference between the measured fluorescence intensity at time 0 and at the time of monochromator crossing that wavelength (Circles). Solid line represents the difference spectrum between time zero and monochromator scanning time, obtained by locally weighted polynomial fitting.

following. After focusing a cell nucleus and recording the dark currents, as previously described, the AOM driver and the monochromator scan were activated. The spectra taken over three different nuclei were averaged point by point and 75 readings were averaged per nanometre interval. The resulting spectra were corrected for instrumental response (Fig. 2) using a reference lamp (Galassi, 1992). A full scan from 468 to 760 nm takes 18 s, each wavelength being crossed by the monochromator scan at time t_w after illumination onset. In order to obtain from the spectrum S_d (distorted by photobleaching) the undistorted S_o spectrum at time t_o, data taken at fixed wavelengths were used: for each wavelength, the relative difference between the fluorescence intensity at time 0 and the fluorescence intensity at the time t_W of monochromator crossing that wavelength was determined. From these values a difference spectrum, correlated with the monochromator scan time, was obtained, with which the distortion was corrected (Fig. 3). By the same means, spectra at any time between 0 and 40 s could be built up.

RESULTS

The curves in Fig. 4 show that a far higher photoenhancement is present at the shortest wavelengths than in the remainder of the emission spectrum, in the case of nuclei mounted in glycerol. In fact, there is a continuous increase of the photoenhancement from 468 to 495 nm (up to almost one order of magnitude higher than the initial value), after which a progressive decline ensues. Above 600 nm the initial increase lasts for only a few seconds, as it does also for the non-filtered fluorescence curve (curve *no filter*). These curves show a biphasic time course, photobleaching ensuing after the brief photo-enhancement. Absorptance, on the other hand, shows a continuous exponential decline from the beginning of irradiation (from 0.108 to 0.079, i.e. 73 % of the initial value). In table I the initial fluorescence intensities for each of the curves of Fig. 4 are shown.

The variation of the emission spectrum of nuclei mounted in glycerol, during the 40 s of irradiation, is shown in Fig. 5A. Reconstructing the spectra, as described in the previous section, by correcting the distortion of a measured spectrum, is preferable to building the spectra *ex novo* from a number of

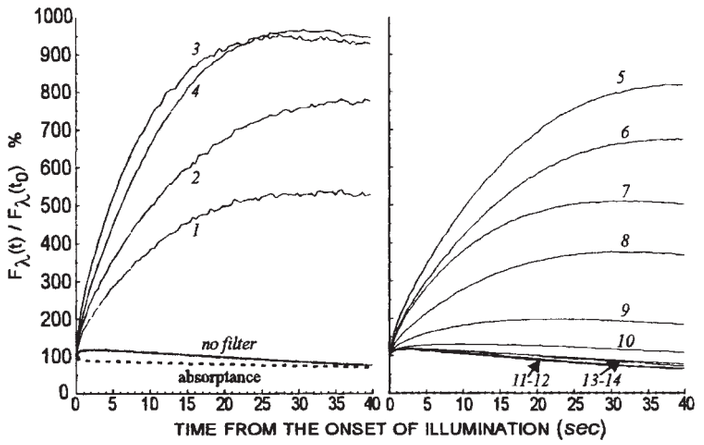

Fig. 4 - Variations of fluorescence and absorptance, expressed as percentage of the initial value measured on nuclei stained with 3 x 10^{-4} M ethidium bromide, mounted in glycerol, after the onset of irradiation with 1.2 $\mu W/\mu m^2$ at 458 nm. Numbering and emission wavelengths as in Table I. The curves have been distributed in two separate panels to avoid confusion from overlapping curves.

measurements taken at fixed wavelengths. The latter procedure would be affected not only by the variability of the time course of fluorescence variation, but also by the variability of the initial fluorescence intensity among nuclei (c.v.≅ 10%). The c.v. of $(F_t(\lambda)-F_{to}(\lambda))/F_{to}(\lambda)$, among three different nuclei on the same slide was found to be always less than 10%. Obviously, similar instantaneous spectra could be obtained, with less effort, if a spectrograph combined with a highly intensifying diode array and a multichannel analyser were available. Fig. 5A shows that the spectral maximum increases above the initial value for the first 10 s, then decreases, and at 40 s is 60% of the initial value. The position of the peak remains at about 607 nm throughout the irradiation period. The difference spectra (Fig. 5B) show that the maximum relative enhancement occurs at 490 nm after 40 s.

Fig. 6A shows the spectra of Fig. 5A corrected for the microspectrophotometer response curve (Fig. 2, Curve 3) and normalised to maximum. The profile, which at the beginning is skewed towards the red side, tends to become more and more symmetrical as the irradiation goes on, because of the increase of the short wavelength component. The FWHM increases from 122 to 130 nm. The bandwidth of the monochromator slit (FWHM: 25 nm) is comparatively small relative to that of ethidium spectra; after deconvolution of the monochromator slit function, a reduction not exceeding 3 per cent of the FWHM was obtained, and no significant shift of the spectrum took place, due to the fairly symmetrical shape of both profiles. The difference spectra (Fig. 6B) show that the increasing short-wavelength component is essentially represented by a band peaking at 485-491 nm.

Fig. 7 refers to nuclei stained with ethidium and mounted in buffer solution. An initial photoenhancement occurs at the shortest wavelengths, as it does in glycerol. However, photobleaching is prevalent here, and above 560 nm only photobleaching is observed. Curves 1–2 (468–475 nm) and 7–9 (525–545 nm) show a triphasic time course, with an initial decrease, followed by enhancement and then by a final decrease. The initial decrease of fluorescence at these wavelengths can be explained by the fact that both intervals lie at the two extremes of the enhancement band. Here the rapid quasi-exponential initial photobleaching prevails over the increase of fluorescence, which at the extremes of the band is relatively small: Only when the time course of photobleaching slows down, can the photoenhancement become predominant. The fluorescence measured without filtering (curve *no filter*) shows a course similar to that of the fluorescence at the longest wavelengths. In fact, the latter wavelengths contribute the largest proportion of intensities to the whole fluorescence spectrun (see Table II).

The absorptance shows an initial increase from 0.115 to 0.138, followed by a decrease down to 0.116, instead of the expected continuous decline reflecting the progressive photo-destruction of the fluorophore. As will be discussed in the following section, the formation of a new strongly absorbing photoproduct is likely to be the cause of the observed increase of absorptance.

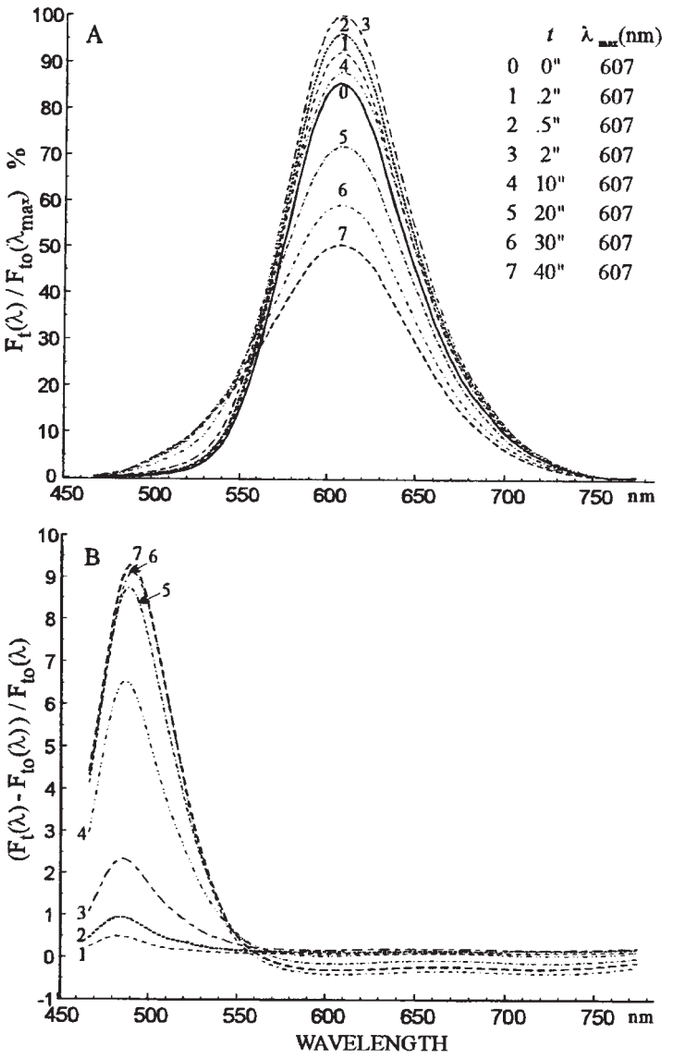

Fig. 5 - A: Emission spectra (uncorrected for instrumental response) of nuclei stained with 3 x 10^{-4} M ethidium bromide, mounted in glycerol at different times after the onset of irradiation with 1.2 μW/μm² at 458 nm. **B**: - Difference spectra *vs*. time zero.

The changes occurring in the emission spectrum during the first 40 s of irradiation of nuclei mounted in phosphate buffer are shown in Fig. 8A. The maximum decreases continuously down to less than 10% of the initial value, while its position shifts from 603 to 599 nm. Fig. 9A shows the spectra of Fig. 8A, corrected for instrumental response curve and normalised to peak amplitude. The broadening of the profile on both sides is substantial, the FWHM increasing from 114 to 173 nm. The peak shifts from 613 to 616 nm. The difference spectra (Fig. 9B) show that the short-wavelength component which undergoes enhancement is essentially represented by a band peaking here at ca. 496 nm., as in the case of glycerol-mounted nuclei,

DISCUSSION

In a previous study it was found that the fluorescence of nuclei stained with ethidium bromide mounted in glycerol is increased at the beginning of irradiation, the photo-enhancement increasing

Table I
Initial fluorescence intensity (arbitrary units) of nuclei mounted in glycerol at different wavelength (nm) or with no filtering.
Numbering as in Fig. 4

	1	2	3	4	5	6	7	8	9	10	11	12	13	14	no filter
filter λ	468	475	485	495	505	515	525	535	545	560	600	670	710	750	-
Fluoresc. (a.u.)	4.1	7.9	11,8	35.3	66.5	98.6	150	283	680	1730	3900	1220	248	34.7	62400

Table II
Initial fluorescence intensity (arbitrary units) of nuclei mounted in buffer at different wavelength (nm) or with no filtering.
Numbering as in Fig. 7

	1	2	3	4	5	6	7	8	9	10	11	12	13	14	no filter
filter λ	468	475	485	495	505	515	525	535	545	560	600	670	710	750	-
Fluoresc. (a.u.)	3.5	6.9	11.7	29.3	58.5	108	200	318	880	2260	4020	1290	204	19.9	64300

with increasing concentration of the staining solution. No similar enhancement was observed in ethidium-stained nuclei mounted in buffer solution (Galassi, 1996). In that study only variations in total fluorescence emission were monitored. In the present study the variation of fluorescence during irradiation has been monitored at specific wavelengths throughout the emission spectrum, and it was found that the variation of fluorescence is dependent on wavelength. When glycerol is used as a mountant, photo-enhancement occurs at all wavelengths (Figures 4–5), and it is favoured at shorter wavelengths. In buffer solution a photo-enhancement is observed only at the shorter wavelengths, though more limited than in glycerol (Figures 7-8). When the spectra are corrected and normalised to maximum (Figures 6 and 9), so as to eliminate the effects of the concurrent photobleaching, the full extent of the photo-enhancement of the short-wavelength band appears, and it is found to be more significant in buffer than in glycerol. It appears that the difference between the time course of fluorescence variation in buffer and glycerol depends largely on the lower photobleaching rate in glycerol.

It was previously assumed that the photo-enhancement was caused principally by concentration dequenching, and to some extent also by attenuation of the inner-filter effect (Galassi, 1996). However, the present finding of a wavelength dependence of fluorescence enhancement makes those explanations not entirely adequate.

The attenuation of the inner-filter effect, accompanying photo-destruction, affects principally the shorter wavelength tail of the spectrum, where overlapping of the emission and absorption spectrum is more significant. In epi-illumination microscopy, the fluorescence intensity in the presence of an inner-filter effect, caused only by the fluorescing species (Rigler, 1966; Prenna *et al.*, 1974), is given by:

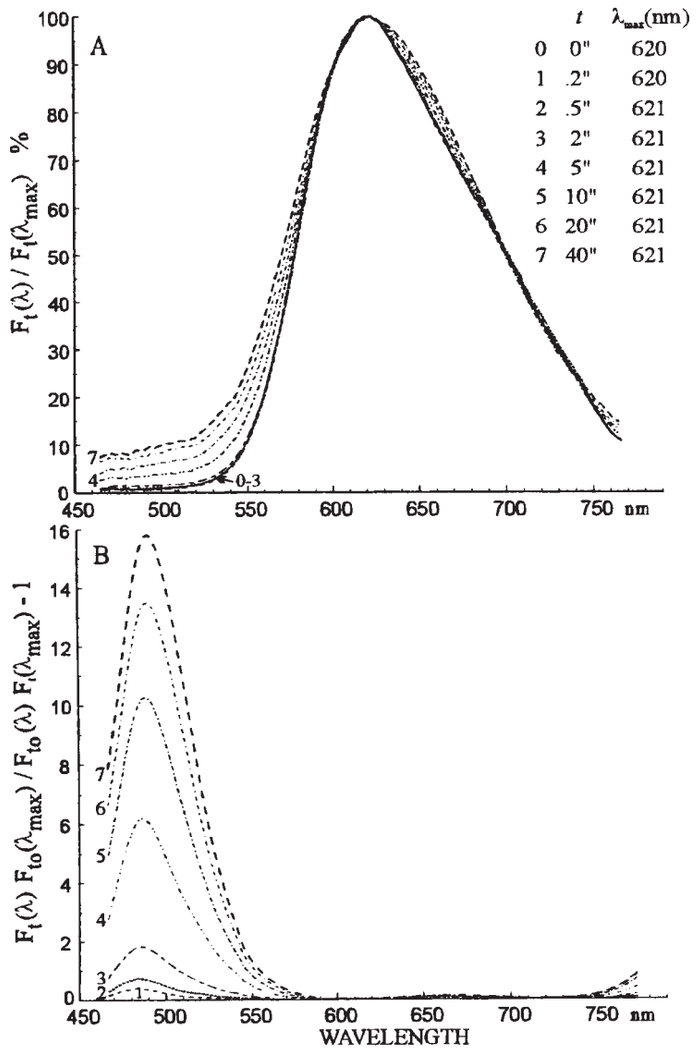

Fig. 6 - A: Emission spectra corrected for instrumental response and with the maximum normalised to 100, to show the variation of the spectral profile at different times after the onset of irradiation with 1.2 μW/μm² at 458 nm. Nuclei stained with 3 x 10^{-4} M ethidium bromide, mounted in glycerol. **B**: - Difference spectra *vs.* time zero.

$$F = \Psi I \frac{E_{\lambda ex_m}}{E_{\lambda ex_m} + E_{\lambda em_m}} \left(1 - e^{-2.3\left(E_{\lambda ex_m} + E_{\lambda em_m}\right)}\right)$$

where $E_{\lambda em_m}$ and $E_{\lambda ex_m}$ are the extinctions of the fluorescing species (i.e. the monomer), at the excitation and emission wavelengths respectively. When a non-fluorescent absorbing species is also present, the fluorescent intensity is given by:

$$F = \Psi I \frac{E_{\lambda ex_m}}{E_{\lambda ex_m} + E_{\lambda ex_d} + E_{\lambda em_m} + E_{\lambda em_d}} \left(1 - e^{-2.3\left(E_{\lambda ex_m} + E_{\lambda ex_d} + E_{\lambda em_m} + E_{\lambda em_d}\right)}\right)$$

where $E_{\lambda em_d}$ and $E_{\lambda ex_d}$ are the extinctions of the non-fluorescing species (ethidium dimers or aggregates), at the excitation and emission wavelengths respectively. Simple numerical calculations were done to see to what extent attenuation of the inner-filter effect can bring about an enhancement of fluorescence. Even assuming extinction values of 0.1, at the excitation and emission wavelengths, (with a ratio of the contribution to extinction of dimer to monomer calculated according to Guenza and Cuniberti, 1988) and further assuming a rate of photo-destruction of the dimer double of that of the monomer, an inner-filter effect not exceeding a few percentage of the fluorescence increase at the shorter wavelength can be calculated.

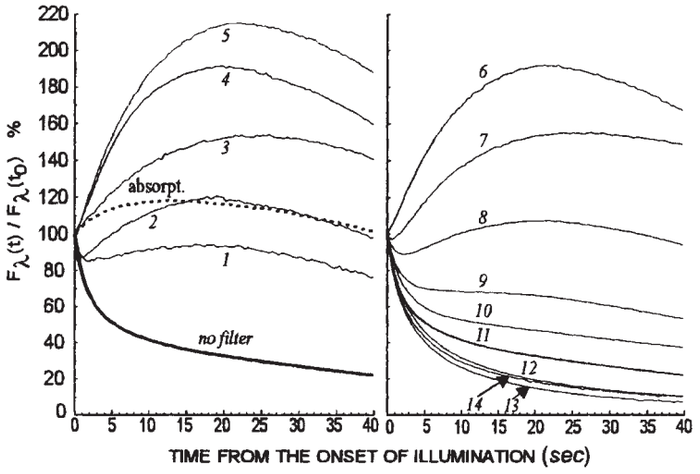

Fig. 7 - Variations of fluorescence and absorptance, expressed as percentage of the initial value measured on nuclei stained with 3 x 10^{-4} M ethidium bromide, mounted in phosphate buffer pH 7.0, after the onset of irradiation with 1.2 $\mu W/\mu m^2$ at 458 nm. Numbering and emission wavelengths as in Table I. The curves have been distributed in two separate panels to avoid confusion from overlapping curves.

Data relative to the variations of the fluorescence maxima and of the spectral bandwidth of DNA-bound versus free ethidium in buffer solution are given in the papers by Bittman (1969) Angerer and Moudrianakis (1972). When the dye binds to DNA or deoxyribonucleoproteins in solution, the emission maximum shifts from 645 nm to 630 nm at low P/D (phosphate/dye) ratios and to 613 nm at high P/D ratios with concomitant narrowing of the FWHM from 166 nm to 130 and 150 nm respectively. Ethidium intercalates into DNA at high P/D ratios, while at low ratios external binding also takes place. Although a P/D ratio cannot be assessed in the case of highly compacted DNA inside nuclei in a staining bath, the relatively high concentration of ethidium used in the present study is consistent with an extensive external binding. This secondary type of binding has been attributed to electrostatic attraction to phosphate groups (Le Pecq and Paoletti, 1967) or to dye stacking of the type occurring with acridine dyes (Waring, 1965, Porumb,1978). A moderate redshift of the maximum (620 to 621 nm in glycerol, 613 to 616 nm in buffer) and a broadening of the FWHM (122 to 130 nm in glycerol, 114 to 173 nm in buffer) observed in the present study might suggest the partial unbinding of ethidium from DNA. This is consistent with the photo-enhancement of fluorescence, if it assumed that only the externally bound ethidium is released, thus allowing the fluorescence of the intercalated dye to be dequenched. However it does not explain the major enhancement at the shorter wavelengths.

West and Lorinez (1974) observed light-induced fluorescence enhancement in leukocytes stained with acridine orange and mounted in buffered saline when the emission was measured at 530 nm, but not when measured at 660 nm. The monomeric and dimeric forms of acridine orange have distinctly separated fluorescence bands, in the green and red regions respectively. Accordingly, photo-destruction would diminish the amount of the dimeric red fluorescing metachromatic species, while the concomitant concentration dequenching would enhance the orthochromatic fluorescence of the monomer. However, no distinct fluorescent bands exist for the monomer and dimer of ethidium. Indeed, the dimer, at least in water, was assumed to be non fluorescent by Guenza and Cuniberti (1988), since no red shift or increase of the bandwidth of the emission spectrum of concentrated ethidium solutions was observed, as was expected for dimers with red-shifted absorption spectrum according to the exciton theory. In conclusion, while that portion of the initial enhancement which affects all wavelengths could indeed be ascribed to concentration dequenching of fluorescence, caused either by light-induced unstacking of the fluorophore, or by photo-destruction-dependent decrease of concentration, the conspicuous enhancement affecting the shorter wavelength tail of the emission spectrum remains at the time unexplained.

The initial fluorescence intensity of ethidium bromide-stained nuclei in glycerol is not significantly different from that in buffer (Tables I and II). Since

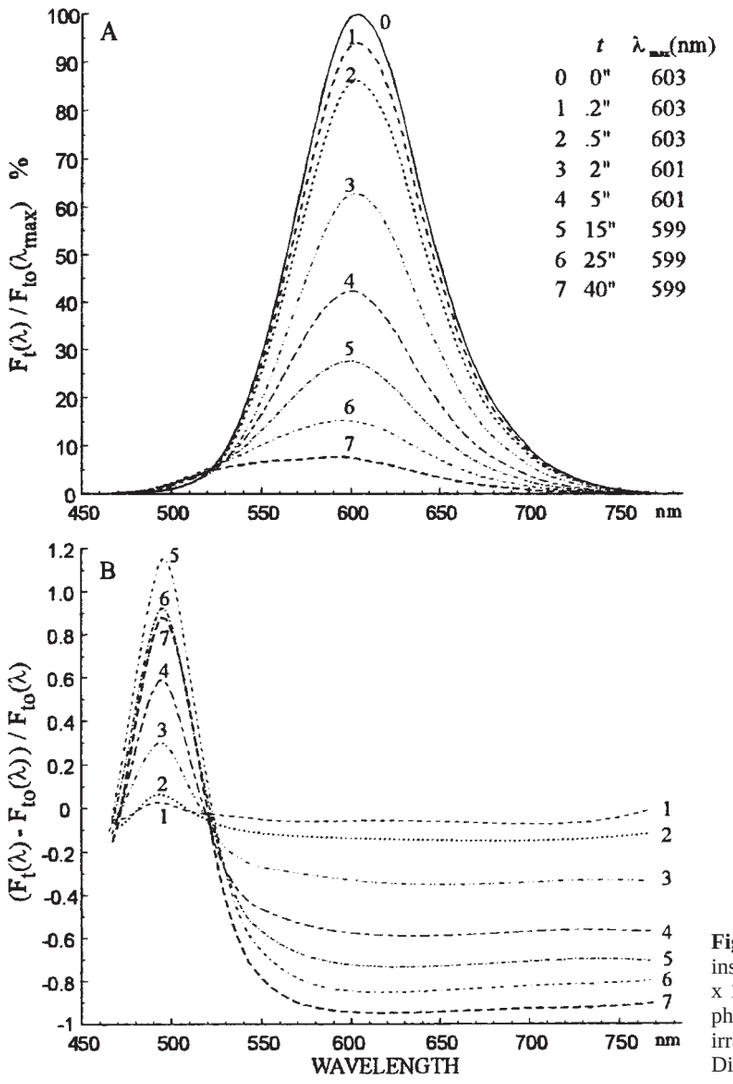

Fig. 8 - A: Emission spectra (uncorrected for instrumental response) of nuclei stained with 3 x 10^{-4} M ethidium bromide, mounted in phosphate buffer, at different times after the onset of irradiation with 1.2 μW/μm² at 458 nm. **B**: - Difference spectra *vs.* time zero.

the intensity of fluorescence of ethidium in different solvents was found to be linearly related to the fluorescence lifetime (Olmsted and Kearns, 1977), it ensues that the fluorescence lifetime of DNA-bound ethidium is not significantly different in glycerol and water, unlike free ethidium which in glycerol has a fluorescence lifetime three times that of ethidium in water (Olmsted and Kearns, 1977). According to Olmsted and Kearns (1977) the low fluorescence lifetime of ethidium in water is caused by proton transfer from the excited molecules of the dye to water molecules and the enhancement of fluorescence on binding to DNA is related to the protection, offered by DNA, from exposure to the solvent. Accordingly it appears that the similarity of fluorescence lifetime of DNA-bound ethidium in glycerol and water is due to the exclusion of both solvents from accessing the proton donating groups of ethidium, when it is bound to the DNA double helix.

The formation of highly absorbing photoproduct(s) seems likely to be the cause of the remarkable initial increase of absorptance observed when buffer was used as a mountant. Magde *et al.* (1974) observed

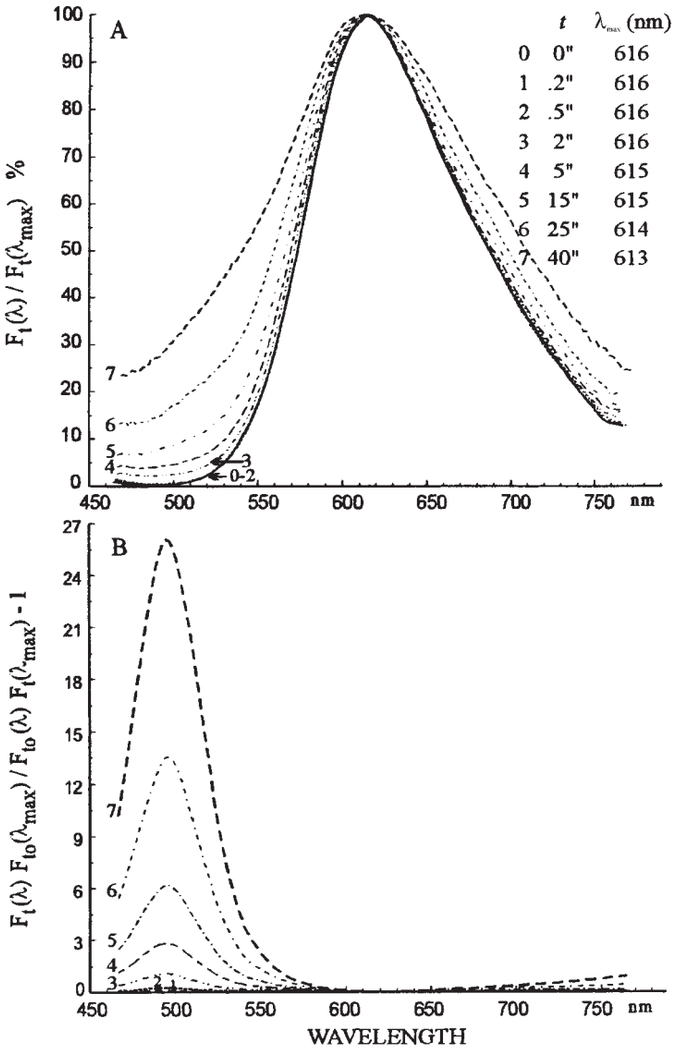

Fig. 9 - **A**: Emission spectra corrected for instrumental response and with the maximum normalised to 100, to show the variation of the spectral profile at different times after the onset of irradiation with 1.2 μW/μm² at 458 nm. Nuclei stained with 3 x 10^{-4} M ethidium bromide, mounted in phosphate buffer. **B**: - Difference spectra *vs.* time zero.

the appearance of a broad absorption band centred at wavelengths lower than the absorption maximum of ethidium, following photobleaching of a solution of the dye and the formation of several different photoproducts was revealed after chromatographic separation. In the present study no increase of absorptance was observed in glycerol and hence no formation of photoproducts seems to occur in this mountant. Further studies are necessary to assess which of the differing physical constants (e.g. viscosity, proton affinity, dielectric constant) is relevant to the observed photophysical and photochemical differences of ethidium in the two solvents (i.e. different bleaching rate and formation of photoproducts).

REFERENCES

Ambroz M., MacRobert A.J., Morgan J., G. Rumbles G., Foley M.S.C, and Phillips D.: Time-resolved fluorescence spectroscopy and intracellular imaging of disulphonated aluminum phthalocyanine. J. Photochem. Photobiol. B: Biol. *22*, 105-117, 1994.

Angerer L.M., and Moudrianakis E.N.: Interaction of ethidium bromide with whole and deproteinized deoxyribonucleoprotein from calf thymus. J. Mol. Biol. *63*, 505-521, 1972.

Azizi F., and Wahl P.: Fluorescence recovery after photobleaching (FRAP) of a fluorescent transferrin internalized in the late transferrin endocytic compartment of living A431 cells: Experiments. *B.B.A. 1327*, 75-88, 1997.

Benson D.M., Bryan J., Plant A.L., Gotto A.M., and Smith L.C: Digital imaging fluorescence microscopy: spatial heterogeneity of photobleaching rate constants in individual cells. J. Cell. Biol. *100*, 1309-1323, 1985.

Bezdetnaya L., Zeghari N., Belitchenko I., Barberi-Heyob M., Merlin J.L., Potapenko A., and Guillemin F.: Spectroscopic and biological testing of photobleaching of porphyrins in solution. Photochem. Photobiol. *64*, 382-386, 1996.

Bilitchenko I., Melnikova V., Bezdetnaya L., Rezzoug H., Merlin J.L., Potapenko A., and Guillemin F.: Characterization of photodegradation of meta-tetra (hydroxyphenyl)chlorin (mTHPC) in solution: Biological consequences in human tumour cells. Photochem. Photobiol. *67*, 584-590, 1998.

Bittman R.: Studies of the binding of ethidium bromide to transfer ribonucleic acid: absorption, fluorescence, ultracentrifugation and kinetic investigations. J. Mol. Biol. 46, 251-268, 1969.

Bjarneson D.W., and Petersen N.O.: Effects of second order photobleaching on recovered diffusion parameters from fluorescence photobleaching recovery. Biophys. J. *60*, 1128-1131, 1991.

Brakenhoff G.J., Visscher K., and Gijsbers E.J.: Fluorescence bleach rate imaging. J. Microsc. *175*, 154-161, 1994.

Enerback L.: Berberine sulphate binding to mast cell polyanions: A cytofluorimetric method for the quantitation of heparin. Histochemistry *42*, 301-313, 1974.

Galassi L.: Fluorescence discrimination in a reflecting environment. J. Microsc. *157*, 181-186, 1990.

Galassi L.: Correction of emission spectra in microspectrofluorimetry using a reference lamp: computations. Eur. J. Histochem. *36*, 243-250, 1992.

Galassi L.: Ethidium bromide fluorescence photo-enhancement in glycerol. Eur. J. Histochem. *40*, 323-330, 1996.

Guenza M., and Cuniberti C.: The ethidium bromide dimer. Absorption and fluorescence properties in aqueous solutions. Spectrochim. Acta *44A*, 1359-1364, 1988.

LePecq J.B., and Paoletti C.: A fluorescent complex between ethidium bromide and nucleic acids. Physical-chemical characterisation. J. Mol. Biol. *27*, 87-106, 1967.

Magde D., Elson E.L., and Webb W.W.: Fluorescence correlation spectroscopy. II. An experimental realization. Biopolymers *13*, 29-61, 1974.

Olmsted J., and Kearns D.R.: Mechanism of ethidium bromide fluorescence enhancement on binding to nucleic acids. Biochemistry *16*, 3647-3654, 1977.

Periasamy N., Bicknese S., and Verkman A.S: Reversible photobleaching of fluorescein conjugates in air-saturated viscous solutions: singlet and triplet state quenching by tryptophan. Photochem. Photobiol. *63*, 265-271, 1997.

Peng Q., Farrants G.W., Madslien K., Bommer J.C., Moan J., Danielsen H.E., and Nesland J.M.: Subcellular localization, redistribution and photobleaching of sulfonated aluminum phtalocyanines in a human melanoma cell line. Int. J. Cancer *49*, 290-295, 1991.

Porumb H.: The solution spectroscopy of drugs and the drug-nucleic acid interactions. Prog. Biophys. Mol. Biol. *34*, 175-195, 1978.

Prenna G., Mazzini G., and Cova S.: Methodological and instrumental aspects of cytofluorimetry. Histochem. J. *6*, 259-278, 1974.

Rigler R.: Microfluorimetric characterization of intracellular nucleic acids and nucleoproteins by acridine orange. Acta Physiol. Scand. *67* suppl., 1-122, 1966.

Rück A., Hildebrandt C., Köllner T., Schneckenburger H., and Steiner R.: Competition between photobleaching and fluorescence increase of photosensitising porphyrins and tetrasulphonated chloroaluminium-phthalocyanine. J. Photochem. Photobiol. B: Biol. *5*, 311-319, 1990.

Rundquist I., and Enerback L.: Millisecond fading and recovery phenomena in fluorescent biological objects. Histochemistry *47*, 79-87, 1976.

Scalatter B.A., Selvin P.R., Axelrod D., Klein M.P., and Hearst J.E.: A polarized photobleaching study of DNA reorientation in agarose gels. Biochemistry *29*, 4790-4798, 1990.

Severin E. and Ohnemus B.: UV dose-dependent increase in the Hoechst fluorescence intensity of both normal and BrdU-DNA. Histochemistry *74*, 279-291, 1982.

Song L., Hennink E.J., Young I.T., and Tanke H.J.: Photobleaching kinetics of fluorescein in quantitative fluorescence microscopy. Biophys. J. *68*, 2588-2600, 1995.

Song L., Varma C.A.G.O., Verhoeven J.W., and Tanke H.J.: Influence of the triplet excited state on the photobleaching kinetics of fluorescein in microscopy. Biophys. J. *70*, 2959-2968, 1996.

Song L., van Gijlswijk R.P.M., Young I.T., and Tanke H.J.: Influence of fluorochrome labeling density on the photobleaching kinetics of fluorescein in microscopy. Cytometry *27*, 213-223, 1997.

Stout A.L., and Axelrod D.: Reversible binding kinetics of a cytoskeletal protein at the erythrocyte submembrane. Biophys.J. *67*, 1324-1334, 1994.

Stout A.L., and Axelrod D.: Spontaneous recovery of fluorescence by photobleached surface-absorbed proteins. Photochem. Photobiol. *62*, 239-244, 1995.

Szabò jr G., Pine P.S., Weaver J.L., Kasari M., and Aszalos A. Epitope mapping by photobleaching resonance energy transfer measurements using a laser scanning microscope system. Biophys. J. *61*, 661-670, 1992.

Swaminathan R., Bicknese S., Periasamy N., and Verkman A.S: Cytoplasmic viscosity near the cell plasma membrane: Translational diffusion of a small fluorescent solute measured

by total internal reflection-fluorescence photobleaching recovery. Biophys. J. *71*, 1140-1151, 1996.

Swaminathan R., Hoang C.P., and Verkman A.S. Photobleaching recovery and anisotropy decay of green fluorescent protein GFP-S65T in solution and cells: cytoplasmic viscosity probed by green fluorescent protein translational and rotational diffusion. Biophys. J. *72*, 1900-1907, 1997.

Van Oostveldt P., Verhaegen F., and Messens K.: Heterogeneous photobleaching in confocal microscopy caused by differences in refractive index and excitation mode. Cytometry *32*, 137-146, 1998.

Waring M.J.: Complex formation between ethidium bromide and nucleic acids. J. Mol. Biol. *13*, 269-282, 1995.

West S.S., and Lorinez A.E.: Fluorescence molecular probes in fluorescence microspectrophotometry and microspectropolarimetry. In *Quantitative fluorescence techniques in cell biology* (Thaer A.A. ed.), pp. 395-407. Berlin, Springer Verlag, 1973.